THE JOURNAL OF BIOLOGICAL CHEMISTRY VOL. 289, NO. 12, pp. 8413–8419, March 21, 2014

A Critical Role for the Neural Zinc Factor ST18 in Pancreatic β-Cell Apoptosis*

Received for publication, January 31, 2014 Published, JBC Papers in Press, February 7, 2014, DOI 10.1074/jbc.M114.554915

Cyndi Henry[‡], **Anne-Françoise Close**[§1], **and Jean Buteau**[§2]

From the [‡]*Université Laval and the CRIUCPQ, Quebec G1V 4G5, Canada and the* [§]*University of Alberta, Edmonton, Alberta T6G 2E1, Canada*

Background: The biological roles of the neural zinc finger transcription factor ST18 remain elusive.
Results: ST18 expression and activity are increased in cytotoxic conditions in pancreatic β-cells. Overexpression of ST18 causes apoptosis. ST18 knockdown prevents palmitate- and cytokine-induced apoptosis.
Conclusion: ST18 plays a critical role in β-cell apoptosis.
Significance: ST18 could represent a novel therapeutic target in diabetes.

The tumor suppressor gene ST18 was originally characterized as the third member of the neural zinc finger transcription factor family. However, little is known about its biological functions. Herein, we demonstrate that, in the pancreas, ST18 expression is restricted to endocrine cells. The detection of ST18 expression in pancreatic β-cells prompted us to investigate its regulation and its role in β-cell mass and function. We show that ST18 expression and activity are increased by cytotoxic concentrations of fatty acids and cytokines in INS832/13 cells. Furthermore, ST18 is also increased in islets of diet-induced obese animals. Overexpression and RNA interference knockdown studies demonstrate that ST18 induces β-cell apoptosis and curtails β-cell replication. Finally, our data suggest that ST18 impairs insulin secretion. Taken together, our findings indicate that ST18 could represent a novel transcriptional mediator of lipotoxicity and cytokine-induced β-cell death. We suggest that genetic or pharmacologic manipulations of ST18 could help maintain a functional β-cell mass.

Zinc fingers are small structural motifs and one of the most abundant DNA binding structures. They are classified according to the number and position of the cysteine and histidine residues, which are responsible for zinc coordination. The neural zinc finger/myelin transcription factor family comprises three members, namely NZF1 (also known as MyT1L), MyT1 (also known as NZF2), and suppression of tumorigenicity 18 (ST18, also known as NZF3/MyT3). ST18 was characterized based on structural homology with the two other NZF family members (1). Thus, they each harbor six $CX_5CX_{12}HX_4C$ (C2HC) zinc finger motifs arranged in two main clusters and recognize the core consensus element AAAGTTT (1). In contrast to its two paralogs, which have been shown to act both as transcriptional activators and repressors, ST18 has been shown to solely repress transcription of genes containing the NZF binding motif in their promoter (1). This was attributed to the absence of specific acidic and serine/threonine-rich domains that are found in NZF1 and MyT1.

NZF1 and MyT1 have been suggested to play a role in neuronal (2) and endocrine pancreatic (3, 4) development, respectively. Nevertheless, the biological functions of the NZF transcription factors remain elusive. Very little is known about the regulation of ST18 expression, its biological role or its transcriptional targets. Loss of ST18 expression was reported in breast tumors and various breast cancer cell lines (5). Also, ectopic expression of ST18 reduced the tumorigenicity of MCF-7 cells (5), thereby suggesting a role for ST18 in tumor suppression. Furthermore, manipulation of ST18 expression in fibroblasts unraveled its potential proapoptotic and proinflammatory roles (6). ST18 expression was reported in the developing pancreas but its potential role in mature β-cells has never been investigated (4).

In this study, we identify the transcriptional repressor ST18 as a novel regulator of β-cell mass and function. We show that ST18 expression is induced by cytotoxic concentrations of free fatty acids or cytokines. ST18 gain-of-function causes β-cell apoptosis, curtails proliferation, and impairs insulin secretion. Conversely, ST18 knockdown prevents palmitate- and cytokine-induced β-cell apoptosis. These data suggest that ST18 could represent a novel molecular target in diabetes.

EXPERIMENTAL PROCEDURES

Material—RPMI 1640, fetal calf serum, and glutamine were purchased from Invitrogen. All other cell culture reagents were from Sigma.

Commercial PCR Array—ST18 tissue distribution was investigated using a rat TissueScan array from Origene (Rockville, MD), according to the manufacturer's protocol. Each qPCR[3] array contains high quality cDNAs from 46 different tissues. Two pairs of arrays were provided in the kit, and they were probed for actin and ST18 in duplicates.

* This work was supported by the Canadian Institutes of Health Research, Diabète Québec, and Montreal Diabetes Research Center.
[1] Supported by Wallonie-Bruxelles, International.
[2] A Fonds de Recherche en Santé du Québec Junior Investigator and a Canadian Diabetes Association Scholar and supported by a Canadian Institutes of Health Research New Investigator award. To whom correspondence should be addressed: Alberta Diabetes Institute, 5-126B Li Ka Shing Centre, Edmonton, Alberta T6G 2E1, Canada. Tel.: 780-492-8386; E-mail: jbuteau@ualberta.ca.

[3] The abbreviation used is: qPCR, quantitative PCR.

Animals—Animal care and handling were performed in accordance with the Canadian Guide for the Care and Use of Laboratory Animals. All experimental procedures received prior approval of the Laval University animal care committee. C57BL/6J mice were fed a high-fat (60 kcal% fat) or control diet (10 kcal% fat) for 8 weeks (The Jackson Laboratory, Bar Harbor, ME). Pancreas were removed and analyzed by immunofluorescence as described below.

Isolation of Pancreatic Islets—Islets were isolated from male (250 g) Wistar rats. Animals were anesthetized, and the pancreatic duct was perfused with a solution containing 0.7 mg/ml type V collagenase. The pancreas was removed and digested in a 37 °C water bath. Islets were subsequently purified on a Histopaque gradient, hand-picked under a microscope, and cultured in complete RPMI medium.

Cell Culture—INS (832/13) (7) cells (passage 36–60) were grown in RPMI 1640 medium supplemented with 10 mM HEPES, 10% heat-inactivated fetal calf serum, 2 mM L-glutamine, 1 mM sodium pyruvate, and 50 μM β-mercaptoethanol at 37 °C in a humidified 5% CO_2 atmosphere. Cells at 70% confluence were washed with PBS and pre-incubated in serum-free RPMI supplemented with 3 mM glucose and 0.1% bovine serum albumin.

Immunohistochemistry—Cells were seeded onto polylysine-coated coverslips and cultured as described above. Cells were then washed, fixed in paraformaldehyde, and incubated with an anti-ST18 antibody.

Pancreas were fixed in paraformaldehyde and embedded in paraffin. We mounted 10-μm sections on slides and performed immunohistochemistry with a mixture of antibodies comprising anti-ST18 and anti-insulin or anti-glucagon antibodies. Primary antibodies were from Sigma.

Images were acquired on a fully automated fluorescence microscope (Olympus, Markham, ON) equipped with Suveyor and ImagePro Plus software. Densitometry results are reported as mean signal intensity per surface area in the islets.

Electrophoretic Mobility Shift Assay—EMSA was performed as described in (8) with slight modifications. Briefly, 5 μg of protein extracts were incubated with a biotin-labeled probe for 20 min at room temperature. Samples were analyzed on 4% non-denaturing polyacrylamide gels and revealed with streptavidin-HRP. A 50-fold excess of unlabeled oligonucleotide was added to assess the specificity of the binding.

Western Blot—Proteins were extracted and quantified by BCA assay (Roche Applied Science) prior to fractionation on 4–12% polyacrylamide gels (Invitrogen).

Transfection—DNA vectors were introduced into INS832/13 cells by nucleofection (Lonza, Mississauga, ON) at a concentration of 5 μg of DNA for 6×10^6 cells. Cells were assayed the following day.

siRNA-mediated Knockdown—ST18-specific stealth siRNAs were purchased from Invitrogen and were transfected with Lipofectamine RNAiMax following the manufacturer's protocol. We have used two siRNAs targeting different ST18 sequences (s141450 and s141448).

Human Islets—Human islets were purchased from Prodo Laboratories (Irvine, CA). Islets from three different lean donors, between 45 and 61 years of age and without any history of diabetes or metabolic disorder, were used. Our study was approved by the Human Research Ethics Board at the University of Alberta.

Apoptosis—Apoptosis was assessed by TUNEL assay (DNA fragmentation) using a fluorescein *in situ* cell death detection kit (Roche Applied Science) (9). In brief, INS or human islet cells were seeded onto polylysine-coated coverslips, fixed in paraformaldehyde, permeabilized with 0.1% Triton X-100 in PBS, blocked with 1% BSA, and incubated for 1 h with a TUNEL reaction mix. The coverslips were then washed in PBS and mounted with antifade containing Hoechst. The fluorescence was visualized under a fluorescence microscope at 400× magnification. At least 600 cells were analyzed for each experimental condition.

Proliferation—Proliferation was evaluated using an ELISA-based BrdU incorporation kit (Roche Applied Science) (10). In brief, INS832/13 cells were transfected with the indicated DNA vectors, seeded in 96-well plates at 70% confluence, and incubated overnight in serum-free RPMI medium supplemented with 3 mM glucose and 0.1% BSA. BrdU was added to the culture medium for the last 1 h of the incubation period. Cells were then fixed and incubated with a peroxidase-conjugated anti-BrdU antibody, and the immune complexes were quantified using a spectrophotometer to measure absorbance (Bio-Rad).

Insulin Secretion and Total Insulin Content Assays—Cells were cultured in 24-well plates, washed, and incubated for 30 min in 2.8 mM glucose KRBH buffer before incubation for 30 min at different glucose concentrations (2.8 and 16 mM) or 35 mM KCl to induce cell depolarization. At the end of the incubation, culture medium was collected, centrifuged to remove cells, and assayed for insulin content by radioimmunoassay (Linco, St. Charles, MO). Total insulin content was measured after acid ethanol extraction. Insulin secretion results are presented as % of insulin content to normalize for the loss of β-cells by apoptosis. Insulin contents were normalized to total protein content.

Calculations and Statistics—Data are presented as means ± S.E. Statistical analyses were performed with SPSS using analysis of variance.

RESULTS

Tissue Distribution of the Neural Zinc Finger Transcription Factor ST18—We first established the expression pattern of ST18 using a commercial PCR array (Fig. 1). Our data show that ST18 is broadly expressed with the most abundant expression observed in the thyroid, the spinal cord, the aorta, and the brain. Along the gastrointestinal tract, ST18 was moderately expressed in the stomach, the liver, and the pancreas. It was virtually absent in the intestine.

We next examined the precise tissue distribution of ST18 within the pancreas by immunofluorescence and PCR. Immunostaining of rat pancreas sections indicated that ST18 expression was restricted to the endocrine pancreas (Fig. 2*A*). Indeed, ST18 staining co-localized with both insulin (*top panels*) and glucagon (*lower panels*) but remained undetected in acinar and ductal cells. To further confirm the pancreatic distribution of ST18, we analyzed its expression by PCR in isolated rat islets and acinar tissues. Consistent with our immunostaining analy-

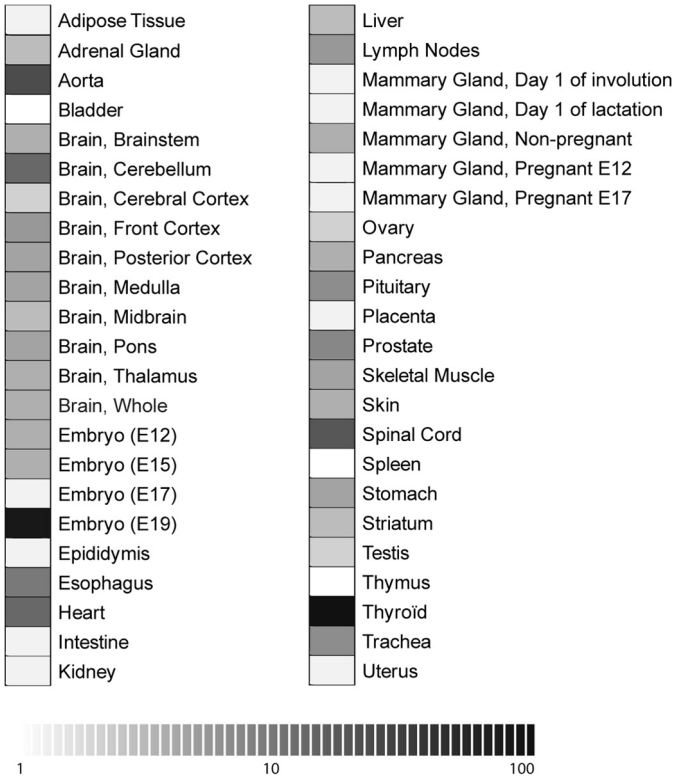

FIGURE 1. **Tissue distribution of ST18.** Relative ST18 expression levels were determined by qPCR using a commercial array. Results are presented on a logarithmic scale.

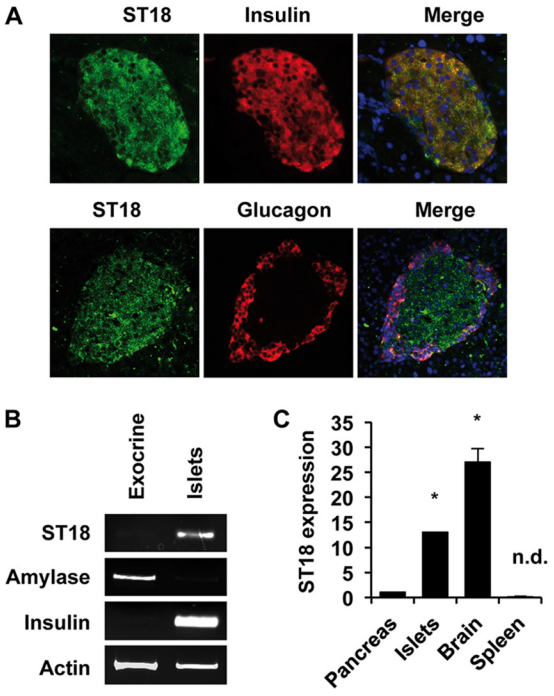

FIGURE 2. **ST18 expression is restricted to endocrine cells in the pancreas.** *A*, double-immunostaining for ST18 (*green*) and insulin or glucagon (*red*). *B*, ST18 expression was investigated by PCR in rat exocrine and islet fractions. Amylase, insulin, and actin were used as controls. Representative images of at least three separate experiments are shown. *C*, quantitative PCR results demonstrating the relative ST18 expression in rat whole pancreas, islets, brain, and spleen. Shown are means ± S.E. of five animals. *, $p < 0.05$ *versus* whole pancreas; *n.d.*, not detected.

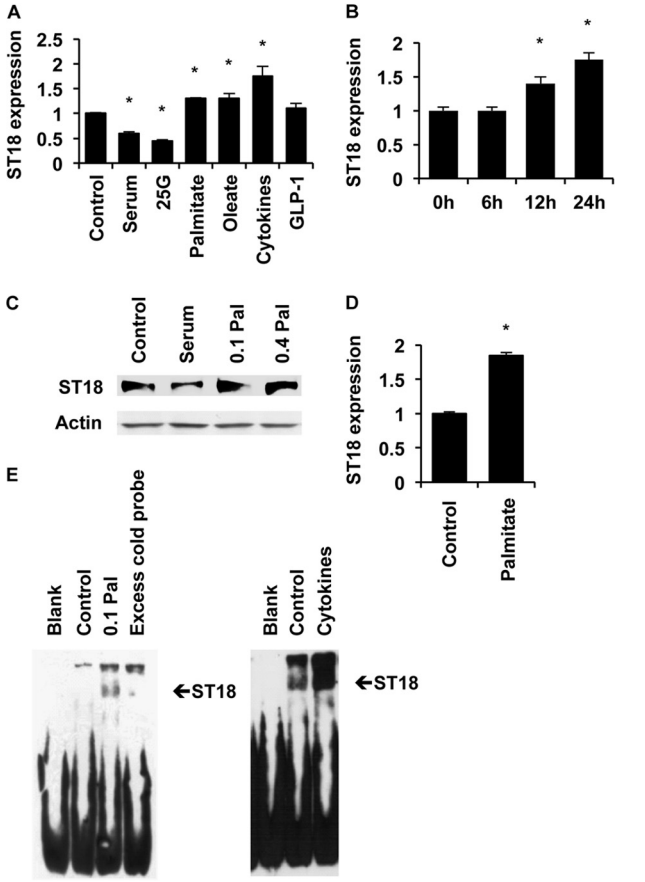

FIGURE 3. **ST18 expression and activity are up-regulated by palmitate or cytokines in INS832/13 cells.** *A*, ST18 expression was investigated by qPCR in INS832/13 cells incubated for 24h in the absence or presence of serum, 25 mM glucose (25G), 0.1 mM palmitate (*Pal*), a cytokine mixture (10 ng/ml IFN-γ and 10 ng/ml IL1β), and 10 nM GLP-1. *B*, qPCR results demonstrating the time-dependent increase in ST18 expression following serum deprivation. *C*, ST18 protein levels were determined by Western blot after overnight incubation in the absence or presence of serum and palmitate (0.1 and 0.4 mM bound to BSA). *D*, ST18 DNA binding activity was evaluated by EMSA. Nuclear extracts were prepared from cells incubated in the presence or absence or palmitate (*left panel*) and cytokines (*right panel*) for 1 h. Shown are means ± S.E. of three experiments, with each comprising duplicates. *, $p < 0.05$ *versus* control. Representative images of at least three separate experiments are shown.

sis, ST18 expression was restricted to the islet fraction, with no expression detected in exocrine cells (Fig. 2*B*). Insulin and amylase were used as controls. Quantification of ST18 expression by real-time qPCR indicated that its expression was ~10-fold higher in isolated islets than in whole pancreas and reached 50% of that in the brain (Fig. 2*C*). ST18 was not detected in the spleen, which was used as a negative control.

Regulation of ST18 Expression and Activity—We next sought to investigate ST18 expression/activity in response to various environmental cues, reasoning that it could provide valuable clues to help grasp its role in β-cells.

We first measured ST18 expression in INS832/13 cells following exposure to 10% serum, elevated glucose, free fatty acids (palmitate and oleate), a cytokine mixture comprising IL1β and IFNγ, or the glucoincretin hormone GLP-1. ST18 expression was significantly increased in the presence of palmitate and oleate as well as cytokines (Fig. 3*A*). Conversely, it was decreased by elevated glucose concentrations. ST18 expression

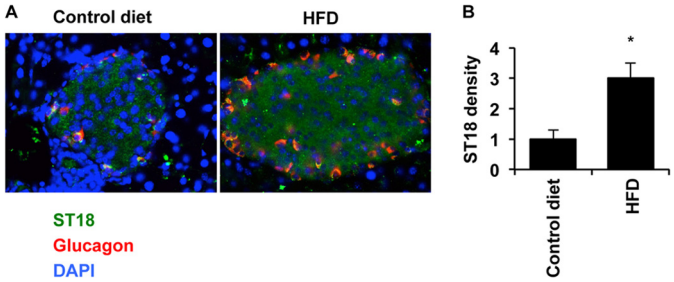

FIGURE 4. **Nuclear localization of ST18 is increased in islets of diet-induced obese animals.** ST18 subcellular localization was investigated by immunofluorescence in pancreas sections from 16-week old mice fed a control or high fat diet (*HFD*). *A*, typical immunofluorescence images are shown. ST18 was stained in *green* and glucagon is colored *red*. Nuclei were counterstained in *blue*. *B*, quantification of ST18 signal intensity in islet cells. Shown are means ± S.E. of four animals for each category. *, $p < 0.05$ *versus* chow diet.

remained unaltered by the glucoincretin hormone GLP-1. In Fig. 3*A*, expression of ST18 was greater in cells incubated in the absence of serum overnight as compared with those incubated with serum. Fig. 3*B* demonstrates that this increase in ST18 expression in serum-deprived cells occurred in a time-dependent manner. Altogether, these observations suggest that conditions deleterious to β-cell function induce ST18 expression.

We next tested whether the rise in ST18 expression translates into increased ST18 protein levels (Fig. 3*C*). Our data show that overnight serum deprivation increased ST18 protein levels in INS cells. Furthermore, the rise in ST18 protein levels was accentuated by cytotoxic concentrations of palmitate (0.4 mM). We next confirmed the effects of palmitate on ST18 expression in normal islet tissue. Thus, isolated human islets exposed to 0.4 mM palmitate overnight displayed a 2-fold increase in ST18 expression as compared with control untreated islets (Fig. 3*D*).

To assess ST18 DNA binding activity, we performed electrophoretic mobility shift assays using a biotin-labeled DNA probe containing an ST18 consensus sequence (1). Our data show that ST18 DNA binding activity was increased by palmitate and cytokines (Fig. 3*E*). The observed shift could be competed with an excess of cold probe. Unfortunately, currently available anti-ST18 antibodies are not suitable for supershift experiments.

We next sought to test whether fatty acids could also induce ST18 expression in islets *in vivo*. ST18 levels were evaluated by immunofluorescence in pancreas sections from diet-induced obese animals. Mice fed a high fat diet (60 kcal% fat) for 12 weeks displayed a significant increase in nuclear ST18 signals compared with control animals fed a 10% fat diet (Fig. 4, *A* and *B*, respectively).

The increase in ST18 expression/activity in response to free fatty acids and cytokines raised the possibility that ST18 could play a role in apoptosis. This prompted us to examine the role of ST18 in lipotoxicity and cytokine-stimulated β-cell death.

The Potential Role of ST18 in β-Cell Apoptosis and Proliferation—We evaluated apoptosis by TUNEL assay in INS832/13 cells with either siRNA-mediated ST18 knockdown or ST18 overexpression. In non-stimulated conditions, gene silencing efficiency was ~70% as measured by qPCR (Fig. 5*A*). A 50% reduction was achieved in the presence of palmitate or cytokines, which completely abolished the rise in ST18 expression and returned its levels to control values (Fig. 5*A*). ST18

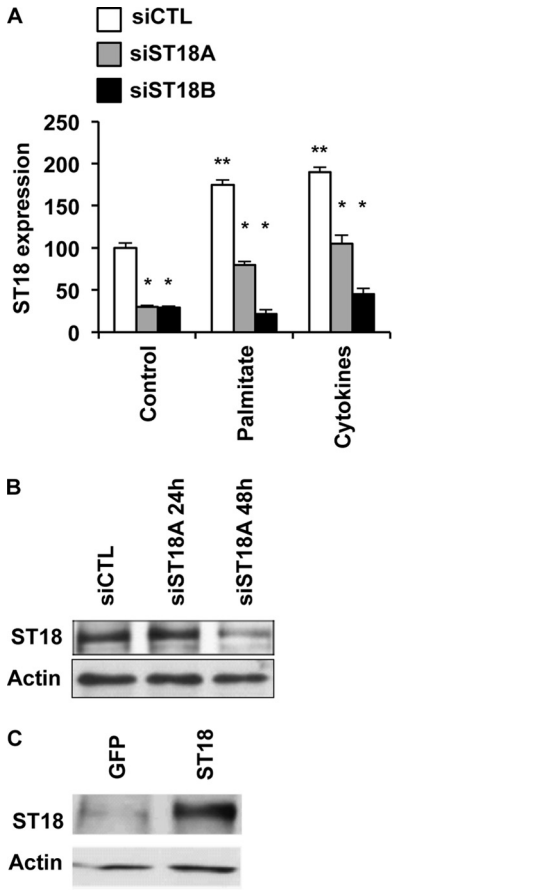

FIGURE 5. **Manipulation of ST18 expression in INS cells.** *A*, INS832/13 cells were transfected with control siRNA (*siCtl*) or two different ST18-specific siRNAs (siST18A and B), and, the following day, were exposed to palmitate (0.1 mM) and cytokines for an additional 24 h. ST18 expression was measured by qPCR. *, $p < 0.05$ *versus* corresponding control siRNA; **, $p < 0.05$ *versus* untreated cells. *B*, ST18 protein levels were determined by Western blot in cells treated as described above in the presence of palmitate. *C*, ST18 protein levels were determined by Western blot in cells transfected with either control (GFP) or pCMV6-ST18 (ST18) vectors for 24 h. Representative images of at least three experiments are shown.

protein levels were assessed by Western blot. In the presence of palmitate, siRNA-mediated ST18 knockdown reduced protein levels by ~70% after 48 h (Fig. 5*B*). Conversely, cells with ST18 gain-of-function displayed a 5- to 10-fold increase in ST18 protein levels (Fig. 5*C*), similarly to what was obtained with elevated concentrations of palmitate as shown in Fig. 3.

Knockdown of ST18 expression significantly decreased β-cell apoptosis caused by serum deprivation and cytotoxic concentrations of palmitate or cytokines (Fig. 6*A*). Conversely, ST18 overexpression caused a marked 4-fold increase in apoptosis, and this effect was not additive to the effect of palmitate (Fig. 6*B*). These data identify ST18 as a novel mediator of lipotoxicity and cytokine-toxicity in β-cells.

We next tested whether the cytotoxic effect of ST18 could be complemented by an inhibitory action on β-cell proliferation. The effect of ST18 on INS832/13 cell proliferation was investigated by BrdU incorporation. ST18 loss-of-function increased proliferation by 30% and prevented the deleterious effect of palmitate (Fig. 6*C*). However, the reduction in proliferation caused by cytokines was unchanged by ST18 knockdown. Consistently with its effect on apoptosis, forced expression of ST18

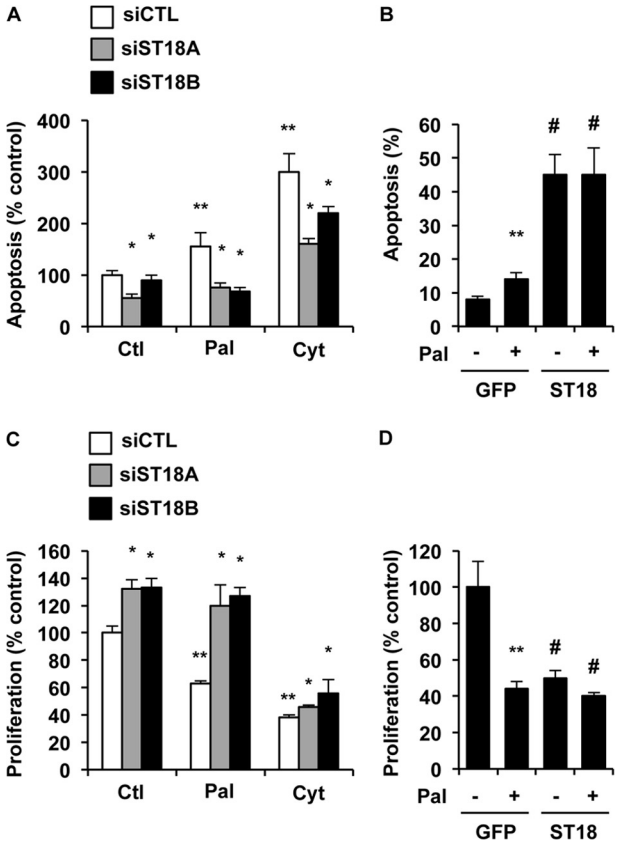

FIGURE 6. **ST18 induces β-cell apoptosis and suppresses proliferation in INS832/13 cells.** *A*, apoptosis was measured by TUNEL assay after overnight incubation in the presence or absence of 0.1 mM palmitate (*Pal*) and cytokines (*Cyt*) in INS832/13 cells transfected with either control siRNAs (*siCTL*) or ST18-specific siRNAs. *B*, Apoptosis was evaluated in the absence or presence of palmitate in INS832/13 cells transfected with control (*Ctl*) GFP or ST18 expression vectors. *C* and *D*, the effects of palmitate and cytokines on proliferation were examined by BrdU incorporation assay in INS832/13 cells with either ST18 loss of function (*C*) or gain of function (*D*), as described above. All results represent means ± S.E. of at least three experiments, each performed in duplicates. *, $p < 0.05$ *versus* control siRNA; **, $p < 0.05$ *versus* untreated cells; #, $p < 0.05$ *versus* control vector.

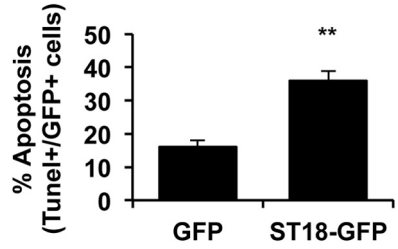

FIGURE 7. **Proapoptotic action of ST18 in isolated human islet cells.** Dispersed human islet cells were transfected with either GFP or ST18-GFP. The following day, apoptotic cells were detected by TUNEL assay. Results show the percentages of TUNEL-positive cells in transfected (*green*) cells. Shown are means ± S.E. of three experiments, each comprising duplicates. *, $p < 0.05$ *versus* GFP control.

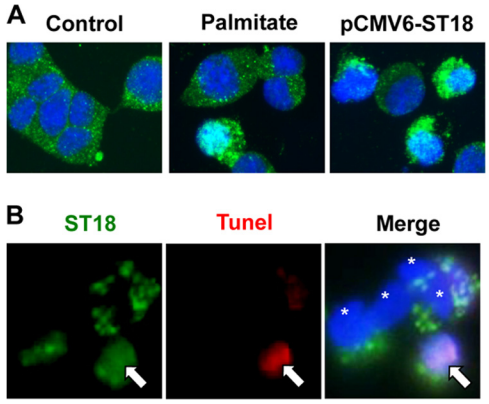

FIGURE 8. **Nuclear localization of ST18 in β-cell apoptosis.** *A*, the subcellular localization of ST18 was investigated by immunofluorescence (*green*) in INS832/13 cells cultured in the absence or presence of palmitate for 24 h, as well as in INS832/13 cells overexpressing ST18. Nuclei are counter-stained in *blue*. Representative images of four separate experiments are shown. *B*, dispersed islet cells were transfected with ST18-GFP and, the following day, apoptotic cells were detected by TUNEL assay (*red*). Healthy cells (*asterisks*) show cytoplasmic localization of ST18, whereas apoptotic cells (*arrow*) display abundant nuclear ST18.

blunted proliferation by 50% and this effect was non-additive to that of palmitate (Fig. 6*D*).

We sought to confirm the proapoptotic action of ST18 in isolated human islet cells. We thus transfected human islet cells with GFP or ST18-GFP and determined the percentage of dead cells in transfected (*green*) cells by Tunel staining. Fig. 7 shows that ST18 gain-of-function induced apoptosis by 2.5-fold in human islet cells. Altogether, our data identify ST18 as a negative regulator of β-cell mass via its combined effect on proliferation and apoptosis.

We next examined the subcellular localization of ST18 by immunofluorescence in the absence or presence of palmitate in INS832/13 cells (Fig. 8). In the control situation, ST18 was predominantly localized in the cytoplasm of INS832/13 cells (Fig. 8*A*, *left panel*). Upon palmitate treatment, the nuclear localization of ST18 increased (Fig. 8*A*, *middle panel*). Forced expression of ST18 also promoted the nuclear translocation of ST18 concomitantly with apoptosis (Fig. 8*A*, *right panel*). We next investigated the subcellular localization of ST18 in dispersed human islet cells using ST18-GFP (Fig. 8*B*). ST18 was found almost exclusively in the cytoplasm of healthy human islet cells (Fig. 8*B*, *asterisks*). However, we detected nuclear ST18 in islet cells undergoing apoptosis (Fig. 8*B*, *white arrow*). Thus, ST18 is predominantly cytoplasmic in unchallenged INS832/13 cells and translocates to the nucleus upon palmitate treatment. ST18 nuclear localization in human islet cells coincides with apoptosis.

ST18 Affects Insulin Secretion by a Distal Mechanism—Finally, we sought to investigate the effect of ST18 on β-cell function by measuring insulin secretion in INS832/13 cells with ST18 overexpression (Fig. 9*A*). ST18 slightly increased basal insulin release and completely abolished both glucose- and KCl-stimulated insulin secretion. The fact that ST18 inhibited the effects of KCl suggests that ST18 could act (at least in part) via a mechanism distal to calcium mobilization. Forced expression of ST18 did not significantly alter insulin content (Fig. 9*B*).

DISCUSSION

ST18 was originally identified in rat brain tissue based on sequence homology with previous members of the NZF family (1). However, very little is known about its biological function as it remains relatively unexplored. Our study is the first to investigate ST18 expression in the pancreas and to functionally characterize ST18 in β-cells.

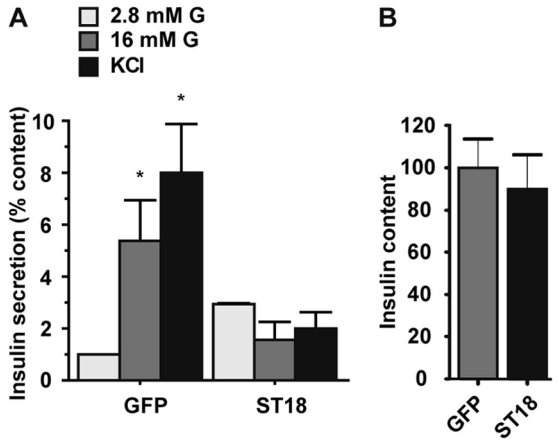

FIGURE 9. **ST18 impairs insulin secretion.** *A*, insulin secretion was determined in INS832/13 cells transfected with either control GFP or ST18 vectors. Cells were incubated at low (2.8 mM) or high (16 mM) glucose (*G*) concentrations, or in the presence of 35 mM KCl to induce cell depolarization. *B*, insulin content was normalized to total protein content and expressed as percent of control. Shown are means ± S.E. of at least three experiments, with each performed in duplicate. *, $p < 0.05$.

We demonstrate that, in the pancreas, ST18 expression is restricted to endocrine cells. We also provide evidence that both ST18 expression and activity are increased by prolonged exposure to free fatty acids and cytokines. This observation is potentially important because hyperlipidemia and cytokine production are common features of both type 1 as well as type 2 diabetes (11) and, collectively, contribute to β-cell demise. Indeed, local production of cytokines within islets induces β-cell apoptosis in type 1 as well as in type 2 diabetes (12), whereas chronic exposure to elevated levels of free fatty acids causes β-cell apoptosis and impairs glucose-stimulated insulin secretion, a phenomenon often referred to as "lipotoxicity" (13, 14). Using siRNA-mediated ST18 knockdown, we herein demonstrate that the proapoptotic action of free fatty acids and cytokines are mediated by ST18 in β-cells.

The proapoptotic action of ST18 is consistent with its role in tumor suppression. ST18 was reported to be down-regulated in breast cancer cell lines and in a majority of breast tumors (5). Also, ectopic ST18 expression in the breast cancer cell line MCF-7 blunted colony formation in soft agar and tumor formation in a xenograft mouse model (5). However, the authors did not specifically measure apoptosis in their system. Another publication demonstrated a proinflammatory role for ST18 in fibroblasts (6). In this study, siRNA-mediated knockdown of ST18 reduced TNFα-induced apoptosis and proinflammatory gene expression, whereas its overexpression significantly enhanced apoptosis. These data, along with ours, support an overarching role of ST18 in cell death. However, the biological role of ST18 is likely to be more complex. A more recent publication reported that ST18 expression was up-regulated during neuronal differentiation *in vitro* and *in vivo* (15). The authors went on to show that forced expression of ST18 in P19 cells (a model of neuronal progenitor cells) caused spontaneous differentiation. The action of ST18 on neuronal differentiation was synergistic to that of the bHLH protein Neurog1. Thus, the biological role of ST18 may be context-dependent.

The role of ST18 in neuronal differentiation is reminiscent of the role of its paralog MyT1 in endocrine cell differentiation. The group of Dr. Gu (4) has shown that MyT1 is required for proper endocrine cell differentiation and that Myt1 and Ngn3 form a feed-forward loop in pancreatic progenitor cells (16). This raises questions about a possible redundancy between all three NZF paralogs. However, the bulk of evidence suggests that NZF members could each exert specific actions: (i) NZF members display different binding affinities for closely related sequences (1); (ii) ST18 acts as a transcriptional repressor on reporter constructs containing a consensus binding element, whereas MyT1 and NZF2 act as transcriptional activators (1); (iii) ST18 lacks acidic and serine/threonine-rich regulatory domains that are present in its two paralogs (1); (iv) and finally, the three NZF members are not equipotent in inducing neuronal differentiation (15).

Unfortunately, the pathways that govern ST18 expression have never been explored. Likewise, its transcriptional targets remain elusive, thereby depriving us from very valuable clues about its mode of action. As more molecular tools and genetically engineered animals are made available, we expect future studies to fill this critical gap in knowledge.

In summary, we characterized ST18 as a transcriptional mediator of lipotoxicity and cytokine-induced β-cell apoptosis. ST18 could therefore represent a common effector of fatty acid- and cytokine-induced β-cell death. We suggest that ST18 could be a potential target for the preservation/regeneration of β-cell mass and function.

Acknowledgments—We thank Renée Paradis for technical assistance and Dr. Yves Deshaies (Laval) for critical reading of the manuscript.

REFERENCES

1. Yee, K. S., and Yu, V. C. (1998) Isolation and characterization of a novel member of the neural zinc finger factor/myelin transcription factor family with transcriptional repression activity. *J. Biol. Chem.* **273,** 5366–5374
2. Kim, J. G., Armstrong, R. C., v. Agoston, D., Robinsky, A., Wiese, C., Nagle, J., and Hudson, L. D. (1997) Myelin transcription factor 1 (Myt1) of the oligodendrocyte lineage, along with a closely related CCHC zinc finger, is expressed in developing neurons in the mammalian central nervous system. *J. Neurosci. Res.* **50,** 272–290
3. Gu, G., Wells, J. M., Dombkowski, D., Preffer, F., Aronow, B., and Melton, D. A. (2004) Global expression analysis of gene regulatory pathways during endocrine pancreatic development. *Development* **131,** 165–179
4. Wang, S., Zhang, J., Zhao, A., Hipkens, S., Magnuson, M. A., and Gu, G. (2007) Loss of Myt1 function partially compromises endocrine islet cell differentiation and pancreatic physiological function in the mouse. *Mech. Dev.* **124,** 898–910
5. Jandrig, B., Seitz, S., Hinzmann, B., Arnold, W., Micheel, B., Koelble, K., Siebert, R., Schwartz, A., Ruecker, K., Schlag, P. M., Scherneck, S., and Rosenthal, A. (2004) ST18 is a breast cancer tumor suppressor gene at human chromosome 8q11.2. *Oncogene* **23,** 9295–9302
6. Yang, J., Siqueira, M. F., Behl, Y., Alikhani, M., and Graves, D. T. (2008) The transcription factor ST18 regulates proapoptotic and proinflammatory gene expression in fibroblasts. *FASEB J.* **22,** 3956–3967
7. Hohmeier, H. E., Mulder, H., Chen, G., Henkel-Rieger, R., Prentki, M., and Newgard, C. B. (2000) Isolation of INS-1-derived cell lines with robust ATP-sensitive K+ channel-dependent and -independent glucose-stimulated insulin secretion. *Diabetes* **49,** 424–430
8. Buteau, J., Roduit, R., Susini, S., and Prentki, M. (1999) Glucagon-like peptide-1 promotes DNA synthesis, activates phosphatidylinositol 3-kinase and increases transcription factor pancreatic and duodenal homeobox gene 1 (PDX-1) DNA binding activity in beta (INS-1)-cells. *Diabetologia* **42,** 856–864

9. Buteau, J., El-Assaad, W., Rhodes, C. J., Rosenberg, L., Joly, E., and Prentki, M. (2004) Glucagon-like peptide-1 prevents β cell glucolipotoxicity. *Diabetologia* **47,** 806–815
10. Buteau, J., Spatz, M. L., and Accili, D. (2006) Transcription factor FoxO1 mediates glucagon-like peptide-1 effects on pancreatic β-cell mass. *Diabetes* **55,** 1190–1196
11. Rhodes, C. J. (2005) Type 2 diabetes-a matter of β-cell life and death? *Science* **307,** 380–384
12. Donath, M. Y., Størling, J., Maedler, K., and Mandrup-Poulsen, T. (2003) Inflammatory mediators and islet β-cell failure: a link between type 1 and type 2 diabetes. *J. Mol. Med.* **81,** 455–470
13. El-Assaad, W., Buteau, J., Peyot, M. L., Nolan, C., Roduit, R., Hardy, S., Joly, E., Dbaibo, G., Rosenberg, L., and Prentki, M. (2003) Saturated fatty acids synergize with elevated glucose to cause pancreatic β-cell death. *Endocrinology* **144,** 4154–4163
14. Poitout, V., and Robertson, R. P. (2002) Secondary β-cell failure in type 2 diabetes–a convergence of glucotoxicity and lipotoxicity. *Endocrinology* **143,** 339–342
15. Kameyama, T., Matsushita, F., Kadokawa, Y., and Marunouchi, T. (2011) Myt/NZF family transcription factors regulate neuronal differentiation of P19 cells. *Neurosci. Lett.* **497,** 74–79
16. Wang, S., Hecksher-Sorensen, J., Xu, Y., Zhao, A., Dor, Y., Rosenberg, L., Serup, P., and Gu, G. (2008) Myt1 and Ngn3 form a feed-forward expression loop to promote endocrine islet cell differentiation. *Dev. Biol.* **317,** 531–540